Vol 16 No 3, March 2007
1009-1963/2007/16(03)/0772-06

Chinese Physics

© 2007 Chin. Phys. Soc.
and IOP Publishing Ltd

Experimental study on imploding characteristics of wire-array Z pinches on Qiangguang-1 facility*

Wang Zhen(王　真)[a)b)], Xu Rong-Kun(徐荣昆)[b)], Yang Jian-Lun(杨建伦)[b)], Hua Xin-Sheng(华欣生)[b)], Li Lin-Bo(李林波)[b)], Xu Ze-Ping(许泽平)[b)], Ning Jia-Min(宁家敏)[b)], and Song Feng-Jun(宋凤军)[b)]

[a)] *Department of Engineering Physics, Tsinghua University, Beijing* 100084, *China*
[b)] *Institute of Nuclear Physics and Chemistry, Mianyang* 621900, *China*

(Received 9 January 2006; revised manuscript received 21 July 2006)

To investigate the imploding characteristics of cylindrical wire array, experiments with load current varying from 1.5 MA to 1.7 MA were carried out on the Qiangguang-1 facility. The complicated temporal-spatial distribution of x-ray radiation was measured by the one-dimensional (1D) x-ray imaging system. Other diagnostic equipments including the x-ray power meter (XRPM) and the time-integrated pinhole camera were used to record time-resolved x-ray power pulse and pinhole x-ray images. Analysis shows that the fast leading edge of the local x-ray radiation pulse is of primary importance in sharpening x-ray power pulse rather than the temporal synchrony and the spatial uniformity of implosion. Experimental results indicated that the better axial imploding synchrony, the faster the increase of x-ray power for an array consisting of 32 tungsten wires of 5 μm diameter than for the others, and the higher the x-ray radiation power with maximal convergence ratio (r_0/r_1) of 10.5. A 'zipper-like' effect of x-ray radiation extending from the anode to the cathode was also observed.

Keywords: wire array, Z pinch, x-ray power, temporal-spatial distribution
PACC: 5270L, 5225L

1. Introduction

Fast Z pinches is an effective way of generating intense x-rays in connection with inertial confinement fusion and other high energy density applications.[1−3] The energy conversion efficiency to soft x-rays is over 15% from a stored electrical energy, which is remarkably high. But the growth of the magnetic Rayleigh–Taylor (RT) instability,[4] which can abruptly terminate the plasma discharge after about ten Alfven transit times,[5] spoils the implosion and limits the enhancement of x-ray power. Much effort[6−11] have being made on mitigating the growth of the RT instability. Sanford and Deeney[1,12] have found that when the wire gap is below a critical value a sharper increase in x-ray power could be obtained. In low-current implosions (1–2 MA), lower mass of load sets a limit to the employment of large number of wires in the cylindrical array. However, to achieve a radial inward velocity of plasma high enough for obtaining high kinetic energy and x-ray power, the radius of the array should not be too small. As a result the wire gap in these experiments exceeds the critical value and no effective merging of wire plasmas was observed. On the MAG-PIE generator (1.4 MA), much attention was paid to the details in the early phase, e.g., wire plasma formation, seeding and growth of the RT instabilities.[13,14] These experiments are of great value in understanding the intricate Z pinches. In our experiments performed on Qiangguang-1 (QG-1) facility located at the Institute of Northwest Nuclear Technology, full width at half maximum (FWHM) of the x-ray power pulse exceeds 20 ns,[15] that largely lies in the complicated temporal-spatial distribution of x-ray radiation resulting from the RT instabilities. To obtain a stable x-ray power pulse as sharp as possible for further physical experiments and other applications, it is necessary to know how the distribution of x-ray radiation exerts influence on the shape of x-ray power pulse. Owing to the flat spectral response of the 1D x-ray imaging system[16] in the range of photon energy from 100 eV to 1.2 keV,[17] in which the major part of x-rays falls, streak images of x-ray radiation can admirably reveal the complicated distribution. With the help of 1D x-ray imaging, study on the effect of the x-ray distribution was carried out while varying the load geometry. As observed in Ref.[16], with the slit parallel or perpendicular to the array axis one can get radial or axial

*Project supported by the National Natural Science Foundation of China (Grant No 10035030).

streak image which is 1D spatio- and time- resolved. In this paper only axial streak images are discussed.

2. Experimental setup

Calculation with the model of infinitely thin shell[18,19] indicates that the QG-1 facility may drive a load comprising 10 to 50 5 μm-diameter tungsten wires with current rising to 1.5 MA in 80 ns. As part of a series of our experiments, characteristics of x-ray radiation was studied by varying the load diameter and increasing the number of wires in the array, and some results have been presented in Ref.[15]. It has been pointed out that the wire array with diameter of 8 mm and length of 20 mm (consisting of 32 tungsten wires of 5 μm diameter) has relatively good performance. In experiments to be discussed in this paper, wire diameter was increased while keeping the diameter and the length of the array constant. Besides the array comprising 32 tungsten wires with wire diameter of 5 μm and 6 μm, the aluminium wire array consisting of 24 15 μm-diameter wires were also used. All these arrays were 20 mm in length and 8 mm in diameter. The streak image of x-ray radiation, which was recorded by the 1D x-ray imaging system, has a spatial resolution of 150 μm and a temporal resolution less than 3 ns that mainly depends on the response of the plastic scintillator film stuck on the fibre array. Time-resolved x-ray power pulse was recorded by the XRPM with the same temporal resolution as the 1D x-ray imaging system. A pinhole camera with axial field of view of 10 mm and radial field of view of 8 mm was used to record time-integrated x-ray images. In addition, a laser probe with spatial resolution of 70 μm and temporal resolution of 0.7 ns was used to record shadowgraphs of stagnated dense plasma. All these equipments were installed in the r–θ plane.

3. Experimental results

Typical axial streak images for the three kinds of load were given in Fig.1. Letters A and C denote the anode and the cathode, respectively. One millimetre in x coordinates corresponds to 8.4 ns, while in y coordinates one millimetre corresponds to 1.84 mm, 2.0 mm and 4.58 mm, respectively, due to the different optical magnification and the use of different fibre array in the 1D x-ray imaging system. Foremost subpeak was observed in most shots at the very start of sweeping, at about −60 ns relative to the time of peak x-ray power. Difference in the intensity of x-ray radiation in the early phase is remarkable for different loads. It is much weaker in implosions of 5 μm tungsten wire array than in other cases. These axial streak images also indicate that the x-ray radiation appeared first near the anode and then moved along the axial direction to the cathode, similar to the 'zipper' in gas-puff and fibre Z pinches.[20,21] In some shots even double peak was observed, first near the anode and then near the cathode.

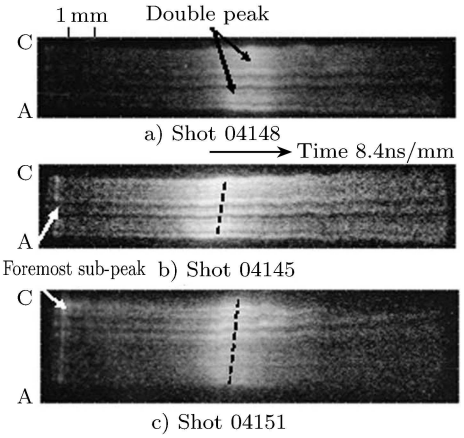


Fig.1. Typical axial streak images for the three loads; dashed lines indicate the 'zipper-like' effect (a) Tungsten wire array of 5 μm wire diameter (b) Aluminium wire array of 15 μm wire diameter (c) Tungsten wire array of 6 μm wire diameter.

Figure 2 shows time-integrated pinhole x-ray images with photon energy $h\nu$>1 keV. The anode blocked some area in Fig.2(a). Discontinuities of hot zones caused by the RT instability were observed in Fig.2(b) and 2(c). For the aluminium wire array, only several discrete hotspots were formed. But for the 5 μm tungsten wire array more hotspots were observed and were distributed uniformly on the axis.

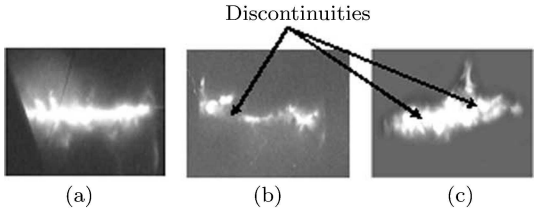


Fig.2. Typical pinhole images of x-ray radiation with photon energy $h\nu$ >1 keV and spatial resolution less than 40 μm. Discontinuities caused by the $m = 0$ instability were observed. (a) Tungsten wire array of 5 μm wire diameter (b) Aluminium wire array of 15 μm wire diameter (c) Tungsten wire array of 6 μm wire diameter.

Shadowgraphs of the on-axis dense plasma are obtained as presented in the following.

4. Discussions

Figure 3 shows the time-resolved x-ray power pulse obtained by the x-rays power meter (XRPM) and similar result derived from the streak image in shot 04148. The two pulses were consistent in shape, taking into consideration the non-linear energy response of the photographic film used in the 1D x-ray imaging system. Double peak with a time interval of 4.8 ns was observed. The earlier one appeared in near-anode area with the amplitude 93.5% of that of the latter one appearing in near-cathode area. However, in the x-ray radiation pulse derived from the streak image, the double peak has a time interval of 5.0 ns and the earlier one is about 91.4% of the latter one in amplitude, which agrees well with the XRPM results. Detailed discussions will be given later.

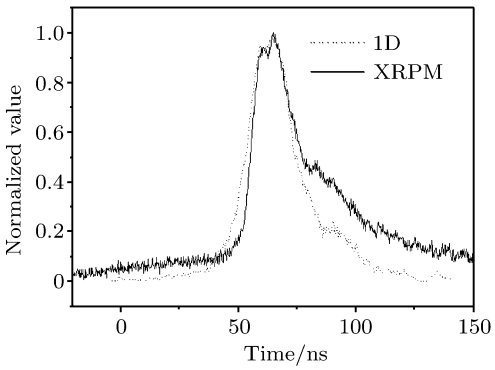
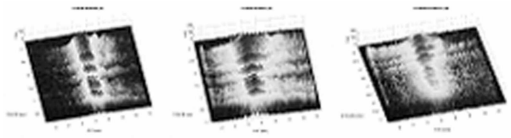


Fig.3. X-ray power pulses in shot 04148; the continuous one is obtained by XRPM and the dashed one derived from integrating the intensity of x-ray radiation with respect to space from the streak image (1D).

Analysis shows that the foremost sub-peak is a result of integrated x-rays on the film in early phase before sweeping. In implosions of the 5 μm tungsten wire array the absence of the sub-peak indicates the much weaker x-ray radiation, e.g., x-ray radiation of the corona and of the precursor plasma. As discussed in Ref.[22], the discharge current is switched to the corona at the very start of applying the current to the wire array and the wire cores prove to be stationary plasma sources during a prolonged period. Area of wire surface decreases as wire diameter decreases. Thus the wire of smaller diameter may produce less low-density plasma and emit weaker x-ray radiation. In addition, the precursor, which is pre-pinched low-density plasma produced by separate wires, also plays an important role. Processed three-dimensional images, as shown in Fig.4, reveal it noticeably and show the fast leading edge of x-ray radiation pulse for the 5μm tungsten wire array.



a) Shot 04148; b) Shot 04145; c) Shot 04151

Fig.4. Reconstructed 3D images (time-spatial-intensity) for the three shots as in Fig.1 and Fig.2.

As aforementioned, more hotspots were observed and were uniformly distributed on the final pinch axis for the 5 μm tungsten wire array. It is empirically known that distribution of hotspots implies the integrity of implosion, i.e., the 5 μm tungsten wire array is better in mitigating the growth of the RT instability. Besides, Ref.[23] says that the viscosity effect of ions also plays an important role with viscosity effect proportional to $m_{\rm i}^{1/2}$. In Ref.[5] growth rate of the RT instability is given as proportional to $n^{-1/2}$, where n is the number of wires comprised the wire array. Therefore mitigating of the instabilities for W wire array is better than for Al wire array. It is in reasonable agreement with experimental results. For the 5 μm and the 6 μm tungsten wire arrays, the difference in the x-ray distribution in the early phase is remarkable. In implosions of the 6 μm tungsten wire array, the precursor was observed before inward acceleration of the majority of load mass. And for the 5 μm tungsten wire array the absence of precursor implies that more load mass will be concentrated on the final imploding when the main current pulse arrives, that may accounts for a better imploding integrity.

Listed in Table 1 are some results for the three kinds of load, including temporal fluctuation of local peak x-ray power and temporal fluctuation of half the peak at the leading edge along the axial direction, corresponding load current and peak x-ray power. The symbols in Table 1 represent number, material and diameter of wires in the array, e.g., 'N24Al15' represents the array comprising 24 aluminium wires with wire diameter of 15μm. Obviously that increasing of x-ray power is for sure the fastest for the 5 μm tungsten wire array. In fact, $\Delta t_{\rm p}$ and $\Delta t_{\rm pw/2}$ in Table 1 may be somewhat exaggerated due to the non-linear energy response of the photographic film. However, the discrepancy between different loads we are concerned with is almost not affected. Besides, the photographic film brings forth a great difficulty in quantifying the intensity of x-ray radiation, so that comparison of x-ray radiation intensity between different shots is quite impracticable.

Table 1. Fluctuation on average for the three loads.

Load	$\Delta t_{\rm p}$/ns	$\Delta t_{\rm pw/2}$/ns	$I_{\rm load}$/MA	$P_{\rm x}$/TW
N24Al15	6.96	6.40	1.67	0.51
N32W6	3.02	4.54	1.66	0.62
N32W5	2.85	2.80	1.57	0.81

As listed in Table 1, for the loads consisting of 15 μm Al wires and of 6 μm W wires, deviations of $\Delta t_{\rm p}$ and P_x are 3.94 ns and 0.11 TW, respectively. And for the loads consisting of 6 μm and 5 μm W wires, the deviations are 0.17 ns and 0.19 TW, respectively. And the value of $\Delta t_{\rm pw/2}$ decreases as the peak x-ray power increases. It seems that the peak x-ray power is not so sensitive to the temporal fluctuation of the x-ray peak ($\Delta t_{\rm p}$) to a certain extent.

In these experiments we have noticed that the local x-ray radiation pulses are similar in shape for different loads except in the early phase. Figure 5 gives some local x-ray radiation pulses for the three kinds of load. Amplitudes of these pulses have been normalized. The fast leading edge of the local x-ray radiation pulse for the 5 μm W wire array is the same as the x-ray power pulse. However, for the other two kinds of loads there is no apparent difference between the leading edges. We also noticed that there is no apparent difference between the falling edges of the three loads. Summing up the discussions in the last three paragraphs, we may conclude that the fast and uniform leading edge of local x-ray radiation pulse should be of primary importance.

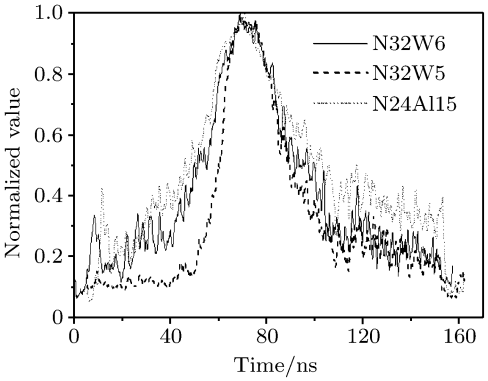


Fig.5. Typical local x-ray radiation pulses for the three loads. Amplitude of the pulses is normalized. Integrating region with size of $\Delta Z = 1$ mm was chosen arbitrarily along the axial direction.

Table 1 also shows that for the loads consisting of 15 μm Al wires and 5 μm W wires $\Delta t_{\rm p}$ is comparable to $\Delta t_{\rm pw/2}$, but for the load of 6 μm W wires $\Delta t_{\rm p}$ is much smaller than $\Delta t_{\rm pw/2}$. This may be attributed to the nonuniform axial distribution of x-ray radiation. Figure 6 and Table 2 give detailed demonstrations. Loads used in the two shots were both the 5 μm tungsten wire array. In Fig.6, the y-coordinates are the normalized intensity of local x-ray radiation ($\Delta Z = 1$ mm). In shot 04147 the x-ray radiation intensity near the anode is 80.0% of that near the cathode, and it is 91.4% in shot 04148. But the value of $\Delta t_{\rm p}$ in shot 04147 is much smaller than that in shot 04148, while the peak x-ray power in shot 04148 is 14.5% higher than that in shot 04147. Figure 6 shows that the leading edges of x-ray radiation pulses are similarly fast. So long as comparison of x-ray radiation intensity between different shots is impracticable, we cannot conclude here decisively whether the nonuniform spatial distribution is responsible. In other words, if intensity of the local x-ray radiation pulse in shot 04147 is no less than that in shot 04148, we can confirm the effect of the axial uniformity and then the improvement in wire quality and symmetry is necessary. If not, then the discussions will be more complicated.

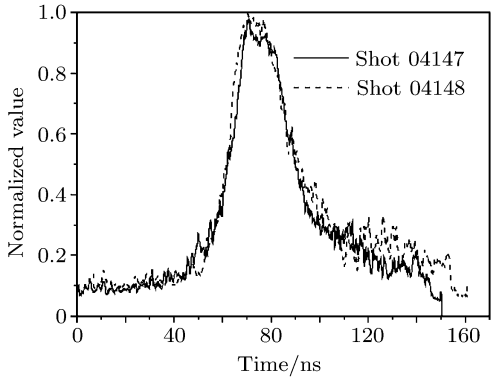


Fig.6. Local x-ray radiation pulses in shot 04147 and shot 04148 under the same conditions as in Fig.5. The pulses agree quite well.

Table 2. Fluctuation for two shots of the same load.

Shot	$\Delta t_{\rm p}$/ns	$\Delta t_{\rm pw/2}$/ns	$I_{\rm load}$/MA	$P_{\rm x}$/TW
04147	2.34	2.73	1.58	0.76
04148	3.34	2.86	1.61	0.86

In these experiments the 'zipper-like effect' extending from the anode to the cathode was observed. In some case the 'zipper' developed into a double peak as in shot 04148. It's well known that such 'zipper' effect of x-ray radiation can widen the x-ray power pulse and lower the peak x-ray power. Figure 7, in which the ordinate stands for the time of x-ray peak and the abscissa stands for the position along the axis,

gives an example of shot 04151. However, we should to point out that the ratio is a mean value of linear fit. In fact the 'zipper' ratios in area near the anode and near the cathode are smaller than that in the middle area along the axis. In some cases the 'zipper' ratio increases rapidly in the middle area, it may be the reason of the formation of the double peak. So that it is difficult to give description to 'zipper-like' effect with linear fit. These results are quite contrary to that in our experiments conducted on the Angara-5-1 facility, and contrary to the results in gas-puff and fibre pinches too. In addition, it is worth noting that in our experiments conducted on QG-1 facility plasma jets from electrodes were observed, which were absent in experiments conducted on the Angara-5-1 facility. It may be attributed to the electric field in areas near the electrodes. On QG-1 facility, fewer wires in the array results in a higher initial impedance, and the load voltage is over 1 MV with load height of 2 cm, but on Angara-5 generator the voltage is about 300 kV with load height of 1.5 cm. Moreover, the structure of electrodes is different as well. On QG-1 facility, the load was installed horizontally, so that annular slots in the electrodes were necessary for the installation of wires. The slots resulted in an enhancement of the local electric field in areas close to the electrodes. Therefore electric field near electrodes on QG-1 facility is much stronger than on Angara-5-1 facility and the plasma jets from area near electrodes were produced. The plasma jets occurred about several nanoseconds before the inward acceleration of the major part of load mass, and disturbed the mass distribution along the pinch axis. Preliminary experiments show that plasma jets were reduced as the width of the slots increased.

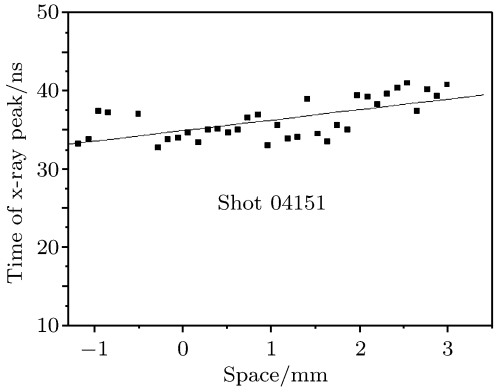


Fig.7. Mean ratio of the 'zipper' in shot 04151 is about 0.30 ns/mm, with consideration that for the abscissa one millimetre corresponds to 4.58 mm with optical magnification factor of 4.58:1.

Further experiments with conical array and with further improvement of electrode structure to mitigate the 'zipper' effect and to reduce plasma jets are under consideration.

Figure 8 gives shadowgraph of the stagnated on-axis plasma close to the time of x-ray peak. Minimal pinch radius r_1 is 0.38 mm measured at −2ns relative to the time of x-ray peak in this shot. With initial array radius r_0 of 4 mm, the convergence ratio r_0/r_1 is about 10.5, about two times greater than the radiative convergence ratio reported in Ref.[15]. Lindl[24] suggests a scaling for the plasma temperature with the peak x-ray power as $kT \propto P_x^{1/4}$, according to which the temperature of plasma at stagnation is about 60 eV with peak x-ray power of about 0.8 TW. Moreover, calculation shows that the tungsten atom was nearly fully ionized with the plasma temperature exceeding 40 eV. Then the mean electron density is $6 \times 10^{21}\mathrm{cm}^{-3}$, which is about three times less than the cut-off limit of the 266 nm laser. It is because that the laser lights are deflected out of the optical system when passing through the plasma regions where the electron density gradient is large enough. Estimation gives a electron density gradient of about $1.8 \times 10^{21}\,\mathrm{cm}^{-3}$ on the edge of the shadow (integrated along the path of laser beam).

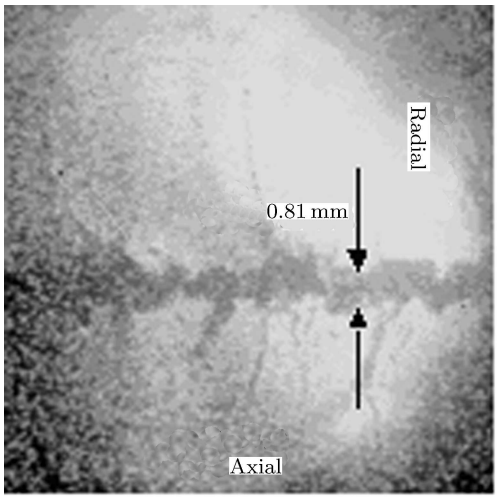


Fig.8. Shadowgraphs of 266 nm laser probing taken at +1ns relative to x-ray peak in shot 05143. Load used in this shot is the 5 μm tungsten wire array. Diameter of the 'on-axis' dense plasma column, i.e. the shadow in the image, is 0.81 mm.

5. Conclusions

The fast leading edge of local x-ray radiation pulse is of primary importance in sharpening x-ray power

pulse rather than the temporal synchrony and spatial uniformity of implosion.

It has better axial imploding integrity for the cylindrical array comprising 32 tungsten wires with diameter of 5 μm, and higher x-ray power with maximal convergence ratio r_0/r_1 of about 10.5.

A 'zipper-like' effect is observed propagating from the anode to the cathode, contrary to the zipper found in gas-puff and fibre Z pinches, for which the plasma jets from the electrodes may be responsible.

Acknowledgments

Thanks to the crew of Qiangguang-1 facility for help in experiments and thanks to Ding Ning for many constructive suggestions.

References

[1] Sanford T W L, Allshouse G O, Marder B M, Nash T J, Mock R C, Spielman R B, Seamen J F, McGurn J S, Jobe D, Gilliland T L, Vargas M, Struve K W, Stygar W A, Douglas M R and Matzen M K 1996 *Phys. Rev. Lett.* **77** 5063

[2] Matzen M K 1997 *Phys. Plasmas* **4** 1519

[3] Deeney C, Nash T J, Spielman R B, Seaman J F, Chandler G C, Struve K W, Porter J L, Stygar W A, Jobe D O, Gilliland T L and Torres J A 1997 *Phys. Rev.* E **56** 5945

[4] Groot J S D, Toor A, Golberg S M and Liberman M A 1996 *Phys. Plasmas* **4** 737

[5] Haines M G 1998 *IEEE Trans. Plasma Sci.* **26** 1275

[6] Sanford T W L, Mock R C, Spielman R B, Peterson D L, Mosher D and Roderick N F 1998 *Phys. Plasmas* **5** 3737

[7] Sanford T W L, Mock R C, Spielman R B, Haines M G, Chittenden J P, Whitney K G, Apruzese J P, Peterson D L, Greenly J B, Sinars D B, Reisman D B and Mosher D 1999 *Phys. Plasmas* **6** 2030

[8] Shumlak U, Nelson B A, Golingo R P, Jackson S L, Crawford E A and Hartog D J D 2003 *Phys. Plasmas* **10** 1683

[9] Rahman H U, Ney P, Rostoker N, Drie A V and Wessel F J 2004 *Phys. Plasmas* **11** 5595

[10] Lemke R W, Bailey J E, Chandler G A, Nash T J, Slutz S A and Mehlhorn T A 2005 *Phys. Plasmas* **12** 012703

[11] Wanex L F, Sotnikov V I and Leboeuf J N 2005 *Phys. Plasmas* **12** 042101

[12] Deeney C, Douglas M R, Spielman R B, Nash T J, Peterson D L, Eplattenier P L, Chandler G A, Seamen J F and Struve K W 1998 *Phys. Rev. Lett.* **81** 4883

[13] Lebedev S V, Mitchell I H, Rossel R A, Bland S N, Chittenden J P, Dangor A E and Haines M G 1998 *Phys. Rev. Lett.* **81** 4152

[14] Lebedev S V, Beg F N, Bland S N, Chittenden J P, Dangor A E, Haines M G, Pikuz S A and Shelkovenko T A 2000 *Phys. Rev. Lett.* **85** 98

[15] Xu R K, Li Z H, Yang J L, Xu Z P, Ding N, Guo C, Jiang S L, Ning J M, Xia G X, Li L B, Song F J and Cheng J C 2005 *Chin. Phys.* **14** 1613

[16] Xu R K, Li Z H, Guo C, Yang J L, Li L B, Song F J, Ning J M, Xia G X and Xu Z P 2003 *Acta Phys. Sin.* **52** 1203 (in Chinese)

[17] Guo C, Xu R K, Li Z H, Xia G X, Ning J M and Song F J 2004 *Acta Phys. Sin.* **53** 1331 (in Chinese)

[18] Ding N, Yang Z H and Ning C 2004 *Acta Phys. Sin.* **53** 808 (in Chinese)

[19] Ning C, Yang Z H and Ding N 2003 *High Power Laser and Particle Beams* **15** 1200 (in Chinese)

[20] Pereira N R and Davis J 1998 *J. Appl. Phys.* **64** R1

[21] Lorenz A, Beg F N, Camacho J R, Worley J and Dangor A E 1998 *Phys. Rev. Lett.* **81** 361

[22] Grabovsky E V, Nedoseev S L, Oleinik G M, Porofeev I Y and Zukakishvili G G 2003 *30th EPS Conf. on Contr. Fusion and Plasma Phys.* **27**A P3.53

[23] Qiu X M, Huang L and Jian G D 2004 *Chin. Phys. Lett.* **21** 689

[24] Lindl J 1995 *Phys. Plasmas* **2** 3933